RESEARCH ARTICLE

Insight into Tri-coordinated Aluminium Species on Ethanol-to-Olefin Conversion over ZSM-5 Zeolites

Zichun Wang,[a,b] Luke A. O'Dell,[c] Xin Zeng,[a] Can Liu,[a] Shufang Zhao,[a] Wenwen Zhang,[b] Marianne Gaborieau,[d] Yijiao Jiang,[b] and Jun Huang*[a]

Abstract: Ethylene, a key chemical in the synthesis of plastics, fibres, rubbers, solvents and many other necessary chemicals, is produced from petroleum- and coal-based industrial chemical processes. Commercial bioethanol is a renewable low-cost feedstock that can be readily converted into ethylene by a dehydration process using solid acids, such as Brønsted acidic H-ZSM-5 zeolites, and thus, it is an ideal candidate to replace petroleum and coal for the sustainable production of ethylene. In this work, strong Lewis acidic extra-framework tri-coordinated Al^{3+} species were introduced into H-ZSM-5 zeolites to improve their catalytic activity. Remarkably, Al^{3+} species working with Brønsted acid sites can accelerate ethanol dehydration at much lower reaction temperature and short unsteady-state period within 1~2 h, compared to > 9 h for those without Al^{3+} species, which can significantly enhance the ethanol dehydration efficiency and reduce the cost. Reaction mechanism studied by solid-state NMR shows that strong Lewis acidic EFAl-Al^{3+} species can collaborate with Brønsted acid sites and promote ethanol dehydration either directly or indirectly via an aromatics-based cycle to produce ethylene.

Introduction

Ethylene as the simplest olefin is the most important feedstock in the chemical industry, for the synthesis of plastics, fibres, rubbers, solvents and many other chemicals.[1] Over 150 million tonnes of ethylene has been produced annually,[2] by the thermal cracking of naphtha or liquefied petroleum gas, as well as coal-based methanol-to-olefine (MTO) process.[3] Recently, crucial environmental issues and the depletion of fossil feedstock drives the increasing efforts to produce ethylene from renewable resources. Commercial bioethanol is a renewable low-cost chemical derived from the fermentation of non-edible lignocellulosic biomass.[4] Bioethanol can be readily converted into ethylene through a simple catalytic dehydration process using solid acid catalysts,[5] and thus, is an ideal candidate for the sustainable production of ethylene. Globally, over 940 million tonnes of bioethanol is anticipated to be produced in 2021 and keeps growing,[6] which can replace the current feedstock and is promising to realize renewable and carbon-free ethylene industry.

Taking advantages of uniform pore structure, high surface area, adjustable acidity, low cost and wide availability, zeolites are more extensively used in alcohol dehydration reactions[7] than other solid acids.[8] The olefins selectivity and the catalyst stability strongly depend on the acidity of the zeolites.[6, 7g, 7i, 9] Brønsted acid sites (BAS) are the catalytically active sites in ethanol dehydration on zeolites, which are protons at bridging OH groups, generated by Al atoms substituting framework silicon atoms.[7c, 10] H-ZSM-5 zeolites with medium acid strength are favourable to promote ethylene production from ethanol over other zeolites,[7g, 7h] while moderate acid sites on ZSM-5 produce propylene[11] and strong acid sites result in secondary reactions of ethylene to generate aromatic hydrocarbons.[7i, 7j] Reaction routes have been proposed for ethylene production from ethanol at BAS as shown in Scheme S1.

The catalytic performance and stability of H-ZSM-5 zeolites can be remarkably enhanced by post-treatment with steam.[7c, 12] For instance, ethylene selectivity increases from 49 % to 99 % at 96-98 % ethanol conversion at 400 °C on steam-treated H-ZSM-5 (Si/Al = 21). Steam treatment is able to generate extra-framework Al (EFAl) species as Lewis acid sites (LAS) in the channels of H-ZSM-5 from the framework dealumination.[10, 13] ^{27}Al MAS NMR can detect most of EFAls with the chemical shifts at ca. 0-15 ppm assigned to EFAl-Al^{VI} and at ca. 30 ppm assigned to EFAl-Al^{V}.[14] In addition, the detailed EFAl species such as $Al(OH)_3$, AlOOH, AlO^+, $Al(OH)_2^+$ and $AlOH^{2+}$ species have been directly identified in dealuminated zeolites by ^{1}H double-quantum magic-angle-spinning (DQ MAS) solid-state NMR[15] and ^{27}Al DQ MAS NMR.[13b, 16] Tri-coordinated Al^{3+} has the largest positive charge and should be of great interest in catalytic reactions as a strong LAS. However, it remains difficult to be detected by conventional one-dimensional (1D) and two-dimensional (2D) ^{1}H and/or ^{27}Al solid-state NMR techniques due to the large quadrupole coupling constants (QCCs) of tri-coordinated Al^{3+} species.[17] Most recently, tri-coordinated EFAl-Al^{3+} species has been indirectly detected by the solid-state NMR combined with probe molecules and theoretical calculation studies.[13a] It shows a higher electron localization and a shorter P-Al bond of the TMP/EFAl-Al^{3+} adsorption complex compared to other TMP/EFAl counterparts and indicating a strong Lewis acid strength among EFAl species.

The strong LAS can take one electron-pair from the reactant. For instance, alcohol can donate OH electron-pair to LAS,[6, 18] and consequently, the very active $CH_3CH_2^+$ carbene ion is generated,[19] which can be stabilized on negative charged framework oxygen O^- to form the ethoxy group as a key intermediates for the ethylene production as shown in Scheme S2. On the Lewis acidic Al defect, methoxy group was directly observed on dealuminated H-Y zeolite after abstracting the

[a] Dr. Zichun Wang, Ms. Xin Zeng, Ms. Can Liu, Dr. Shufang Zhao, Prof. Dr. Jun Huang
Laboratory for Catalysis Engineering, School of Chemical and Biomolecular Engineering & Sydney Nano Institute
The University of Sydney, NSW 2006, Australia
E-mail: jun.huang@sydney.edu.au
[b] Dr. Zichun Wang, Ms. Wenwen Zhang, Dr. Yijiao Jiang
Department of Engineering,
Macquarie University, Sydney, NSW 2109, Australia
[c] Dr. Luke A. O'Dell
Institute for Frontier Materials
Deakin University, Geelong, VIC 3220, Australia
[d] Dr. Marianne Gaborieau
School of Science and Health
Western Sydney University, Parramatta, NSW 2150, Australia

Supporting information for this article is given via a link at the end of the document.((Please delete this text if not appropriate))

electron-pair OH^- from methanol at Lewis acidic EFAl sites.[20] Introducing EFAl-Al^{3+} species into zeolites, therefore, would promote the $CH_3CH_2^+$ carbene ion production and the catalytic performance for the ethanol dehydration. In this work, H-ZSM-5 zeolites with and without tri-coordinated Al^{3+} species were prepared for the systematically studied the effect of Al^{3+} species on the catalytic dehydration of ethanol to ethylene. The local structure and acidity of H-ZSM-5 zeolites were extensively characterized by NH_3-TPD, ^{27}Al, ^{31}P NMR experiments with suitable probe molecules. The presence of dominant invisible tri-coordinated Al^{3+} species upon Al^{3+} ion-exchange has been confirmed by zeolite with/without water adsorption. The densities of surface acid sites were determined by quantitative ^1H NMR experiment combined with ^{31}P NMR experiment. The used catalysts at the unsteady-state period has been analysis by ^{13}C NMR experiment. The possible reaction mechanism and network for the excellent catalytic performance of H-ZSM-5 with EFAl-Al^{3+} species has been proposed.

Results and Discussion

For the systematic study of the effect of EFAl-Al^{3+} species on the catalytic dehydration of ethanol to ethylene, H-ZSM-5 zeolites with (HZ-2) and without (HZ-1) tri-coordinated Al^{3+} species were successfully prepared. The crystal structure of MFI zeolites were confirmed by XRD patterns (Fig. S1).

Local structure and acidity investigations in H-ZSM-5 zeolites, measured by ^{27}Al, ^{31}P, and ^1H NMR. The coordination of Al species in hydrated HZ zeolites was determined by ^{27}Al MAS NMR spectroscopy (Fig. 1). As shown in Fig. 1a, a strong signal at 55 ppm and a weak signal at 0 ppm were observed in hydrated HZ-1, which were assigned to tetra-coordinated aluminum (Al^{IV}) and hexa-coordinated aluminum (Al^{VI}) species, respectively. Al^{IV} species are widely accepted as Al incorporated into the zeolite framework, contributing to the formation of the bridging SiOHAl groups as BAS at the surface, while Al^{VI} species are often associated with the formation of LAS as introduced before. The study of Al behaviour in zeolites under dehydrated state is important since zeolites are often applied in dehydrated states before catalytic reactions to release surface active sites. Upon dehydration, the line shapes of both Al^{IV} and Al^{VI} species became broader (Fig. 1b) due to the increase of C_{QCC}, which is often observed with quadrupolar nuclei, such as Al (I = 2/5) in asymmetric structural environments.[14a]

In the spectrum of hydrated HZ-2 (Fig. 1c), two signals at 55 and 14 ppm were assigned to Al^{IV} and Al^{VI} species, respectively. The broad hump at 32 ppm could be caused by either penta-coordinated aluminum (Al^V) species or distorted Al^{IV} species, and the ^{27}Al MQMAS NMR technique was applied to identify these species (Fig. 2).[14a, 21] In the ^{27}Al MQMAS NMR spectrum, ^{27}Al species with different coordinations can be distinguished according to their isotopic chemical shift along the $F1$ axis. As shown in Fig. 2a, the signal at 32 ppm is well separated and therefore more likely to be Al^V species than distorted Al^{IV} species, which is clearly identified along with Al^{IV} and Al^{VI} species. After dehydration, the signal of Al^V and Al^{VI} species almost disappeared from the spectrum in Fig. 1d. The absence of Al^V and Al^{VI} signals was also observed in Fig. 2b. The absence of all these signals in the dehydrated HZ-2 zeolite indicates that a large amount of invisible tri-coordinated Al^{3+} species was introduced after the Al^{3+} ion exchange process and dehydration.

The larger C_{QCC} of tri-coordinated Al^{3+} species in dehydrated HZ-2 zeolite could result in these species being undetectable by conventional one-dimensional (1D) and two-dimensional (2D) ^{27}Al MQMAS NMR techniques under moderate magnetic field strengths.[22] Partial water adsorption could significantly improve electric field gradient of Al atom in the local structure, leading to the observation of Al species that are invisible in dehydrated states by ^{27}Al MQMAS NMR experiment.[23] Upon partial rehydration, extra-framework Al^V and Al^{VI} species were again observed in Fig. 2c, which is reversible upon heating. Moreover, the signal of Al^{IV} species of the $F2$ projection was narrowed and became symmetric compared to that in the dehydrated state. The reversible Al^V and Al^{VI} species on hydrated HZ-2 zeolite are considered to be caused by rehydration of invisible tri-coordinated Al^{3+} species. With the strong electron deficiency, the Al^{3+} species is able to capture water molecules in a hydrated state due to the strong oxygen affinity of LAS as shown in the inset scheme in Fig. 2, leading to coordination transfer and reducing their C_{QCC} as often reported.[14b, 14c, 24] The dehydration of Al^V and Al^{VI} species is a result of the regeneration of cationic EFAl-Al^{3+} species.

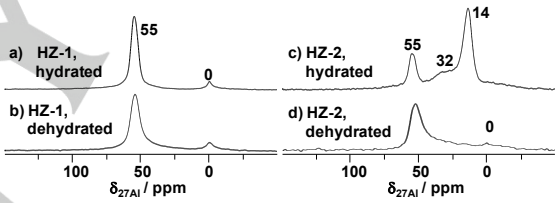

Figure 1. ^{27}Al magic-angle spinning (MAS) NMR spectra hydrated (a, c) and dehydrated (b, d) of HZ-1 (a, b) and HZ-2 (c, d).

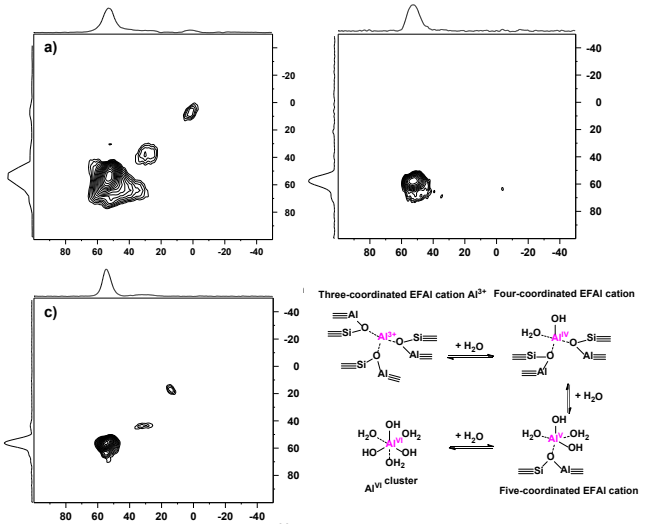

Figure 2. ^{27}Al 3QMAS NMR spectra of hydrated (a), dehydrated (b) and partial rehydrated (c) HZ-2.

When the invisible tri-coordinated Al^{3+} species existed in the dehydrated samples, the LAS can be probed by the guest molecules. ^{31}P MAS NMR spectroscopy is a useful method to determine the type and strength of surface acid sites with TMPO as a probe molecule, and thus it can indirectly distinguish the nature of different Al species.[25] In HZ-1 zeolite, Al^{IV} species is dominant and contributes to the formation of BAS. In Fig. 3a, the ^{31}P signals in the range of 46-73 ppm are caused by protonated TMPO ions at BAS on HZ-1 zeolite, where a more positive chemical shift indicates a higher acid strength of BAS in zeolites. A very weak signal (< 2.5 %) at 38 ppm was also observed, typically for TMPO adsorbed on LAS, which arise from surface Al^{VI} species with a weak signal at δ_{27Al} = 0 ppm in Fig. 1a. In HZ-2 (Fig. 3b), the signal at 38 ppm significantly increased up to 26.3 %, along with another signal of LAS at 32 ppm of 14.8 %. Both signals are attributed to the high content of Al cations, particularly, tri-coordinated Al^{3+} species as revealed in the above ^{27}Al MAS NMR study. Notably, the assignment of the signal at δ_{31P} = 37 ppm was considered as TMPO at LAS by Rakiewicz et al.,[26] however, was not observed with TMPO-loaded γ-Al_2O_3.[27] According to Zheng et al.[28] TMPO is only weakly adsorbed on LAS and is strongly adsorbed on BAS. Upon water loading, LAS tend to form weak BAS and interact with TMPO, however, hydrogen bonded $TMPOH^+$ complexes at BAS are retained. By using hydrated HZ-2, the signals at 38 and 32 ppm in dehydrated HZ-2 were revealed from LAS (Fig. S2). In ^{31}P MAS NMR experiment, each BAS or LAS adsorbed one TMPO molecule in TMPO-loaded HZ-1 and HZ-2 zeolites. Therefore, ^{31}P NMR confirms that HZ-1 contains mainly BAS (> 97.5 %), while HZ-2 zeolite provides a high content of LAS (≈ 54 %) balanced with BAS ((≈ 46 %).

It has been widely accepted that BAS in zeolites are generated by protons compensating the negative charge caused by Al^{IV} species incorporated into the zeolite framework, while Al cations act as LAS.[10, 13a, 29] ^1H MAS NMR experiments were applied to determine surface protons on HZ-1 and HZ-2, such as BAS as catalytic active sites. ^1H MAS NMR spectra of HZ-1 and HZ-2 and corresponding simulation results are shown in Fig. S3. In both zeolites, signals at 3.6~4.8 and 6.5~6.8 ppm were assigned to bridging OH groups and strongly disturbed bridging OH groups via hydroxyl protons interacting with framework oxygens,[10] both are catalytically active BAS on zeolites. After introducing Al^{3+} species and dehydration at 500 °C, the signal at 3.6 ppm in HZ-1 zeolite (Fig. S3a) strongly decreased in HZ-2 zeolite (Fig.S3b). It indicates that the strong dehydration of Al^{3+} hydroxyl species with local BAS contributes to the formation of Al^{3+} species in HZ-2 zeolite, similar as that reported previously.[13b] The strong decrease of surface BAS was further confirmed by the NH_3-TPD analysis as shown in Fig. S4.

Unlike the Brønsted acidic OH groups in amorphous silica-alumina which overlap with terminal SiOH groups at 1.2-2.2 ppm,[30] bridging OH groups (BAS) can be clearly distinguished from non-acidic SiOH groups in zeolites with strong ^1H low-field chemical shifts at 3.6-6.8 ppm (Fig. 4). Therefore, quantitative evaluation of BAS can be achieved with the relative intensity of bridging OH groups in simulating the ^1H MAS NMR spectra of dehydrated HZ-1 and HZ-2 zeolites. Moreover, the density of LAS can be determined by BAS density and the BAS/LAS ratio obtained in ^1H and ^{31}P MAS NMR experiments. The density of BAS and LAS are summarized in Table 1.

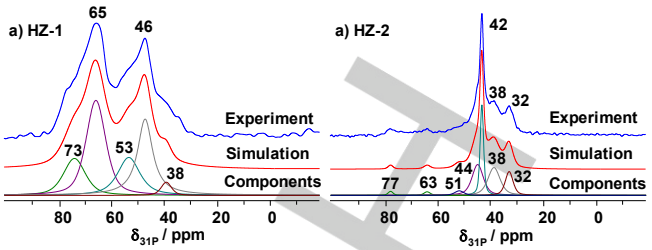

Figure 3. ^{31}P SPE-MAS NMR spectra of dehydrated (500 °C) HZ-1 (a) and HZ-2 (b) zeolites loaded with TMPO.

Table 1. Textural Data and Chemical Composition of H-ZSM-5 Zeolites.

	HZ-1	HZ-2
Brønsted acid sites density (mmol/g)	98.3	48.9
Lewis acid site density (mmol/g)	2.7	57.4

Catalysts Performance. The temperature effect on the catalytic conversion of ethanol over HZ-1 and HZ-2 zeolites was studied in the range of 300-500 °C. As shown in Fig. S5, HZ-1 is less active at low temperature (300 °C), providing an ethanol conversion of ca. 58 % and ethylene selectivity of 86 %. At this temperature, a high selectivity of C_4+ was observed with HZ-1, which may be caused by the low conversion rate of ethanol, leading to ethanol reacting with ethylene. The conversion of ethanol and selectivity to ethylene were significantly enhanced with increasing the reaction temperature from 300°C to 400 °C. At 500 °C, a high selectivity to ethylene (> 95 %) at a nearly complete conversion of ethanol was achieved. Interestingly, HZ-2 with tri-coordinated Al^{3+} species, is highly active through the whole temperature range, providing a high ethylene selectivity (> 95 %) at the complete conversion of ethanol above 300 °C. Obviously, HZ-2 showed the high activity at lower reaction temperatures. As characterization above, HZ-2 has the significant amount of Al^{3+} species as LAS. This is in an agreement with an earlier study[12a] showing that dealuminated H-ZSM-5 zeolite improved the ethylene yield at lower reaction temperature, compared to H-ZSM-5 without EFAl species and Al_2O_3, respectively.

Two reaction mechanisms are suggested for alcohol dehydration in the literature:[31] (1) the concerted water elimination by simultaneous cleavage of the C-OH and C-H bonds of the alcohol via E2 mechanism through the ethoxy group as shown in Scheme S1 BAS-HT, and (2) the cleavage of C-OH bond to form a carbenium ion, which is unstable and can be easily decomposed into ethylene via proton loss, known as E1 mechanism. The formation of primary carbocation intermediates is difficult due to their high energy barrier.[32] The unstable carbenium ions can be evolved into an ethoxy groups by binding to a neighboring oxygen atom, and decomposed into ethylene via a concentrated mechanism as evidenced by IR spectroscopy using isotope-labelled ethanol.[33] Ethoxy groups are widely accepted as the major intermediates in ethanol dehydration on H-form zeolites

(Scheme S1, BAS-HT), which has been directly observed on H-Y zeolite by Wang et al, using ^{13}C NMR spectroscopy.[19b] On alumina (representing LAS), ethylene was mainly formed via a diethyl ether (DEE) intermediate at lower temperatures (Scheme S2a), while a direct dehydration of ethanol to ethylene is preferred at high temperature (> 400 °C) via ethoxy intermediates to provide a high performance.[34]

For HZ-2 with tri-coordinated Al^{3+} species, the BAS density in HZ-2 is significantly lower than HZ-1. Therefore, the distinct high activity of HZ-2 compared to zeolite HZ-1 at low temperature indicates that Al^{3+} species may promote the formation of ethoxy groups over BAS or facilitate the formation of ethoxy groups for ethanol dehydration together with BAS. As shown in Fig. S3, the bridging SiOHAl groups at 3.6 ppm tends to be removed with OH groups induced by Al^{3+} species after dehydration. Therefore, a structure of Al^{3+} species was proposed in Scheme S2b, in line with those proposed in earlier works.[13] The high electron deficient Al^{3+} species are strong LAS compared to other EFAl species and LAS on alumina. DFT calculation study suggested that surface LAS are more effective in the cleavage of C-OH bond than pure BAS.[35] The cleavage of C-OH bond at Al^{3+} sites could result in the formation of ethoxy groups on neighboring Si-O-Al sites. The negative charged Si-O-Al sites are proton acceptors, interacting with H at the primary CH_3- at ethoxy groups and resulting in the decomposition of carbenium ions for ethylene (Scheme S2b). A concerted E2 mechanism was completed via the abstraction of an OH at the Al^{3+} site and a H at a basic Si-O-Al site. More Al^{3+} species and Si-O-Al sites inside zeolites can significant facilitate the conversion of ethanol. The generated Si-OH-Al is able to either act as BAS for ethanol dehydration (Scheme S1, BAS-HT) or react with neighboring AlOH back to EFAl-Al^{3+} species and Si-O-Al sites after dehydration. The latter is confirmed by Deng and co-workers in methanol conversion at 250-300 °C.[20] In that work, EFAl species on dealuminated zeolite H-Y are found to promote the facile generation of methoxy groups through ^{13}C NMR experiments and theoretical calculations, which is unfavourable on zeolite H-Y without EFAl species under the same conditions. Therefore, the presence of high content of strong Lewis acidic tri-coordinated Al^{3+} species here is proposed to accelerate the low-temperature formation of ethoxy groups or very active $CH_3CH_2^+$ carbene ions (Scheme S2b), which are converted into ethylene.

Further studies were carried out at the reaction temperature of 500 °C, highest conversion for both zeolites. The catalytic conversion of ethanol was studied as a function of time on stream (TOS) over H-ZSM-5 zeolites as plotted in Fig. 4. Both catalysts are highly active and achieve a high ethylene selectivity (> 95 %) at complete ethanol conversion, and retained after 22 h reaction time without any activity loss. Over HZ-1 zeolite, ethylene selectivity only increased up to 58 % with 89% ethanol conversion after 2 h reaction time, and reached only 82 % ethylene selectivity at a complete ethanol conversion after 6 h reaction time. After 9 h reaction time, an ethylene selectivity over 90 % was obtained, and gradually increased up to ca. 98 % after 13 h. Interestingly, ethylene selectivity increased sharply to 90 % within the first 2 h reaction time, then increased steadily up to ca. 95 % over HZ-2 zeolite. Obviously, HZ-2 requires much shorter unsteady-state period compared to HZ-1 in obtaining a high ethylene selectivity at steady-state ethanol conversion.

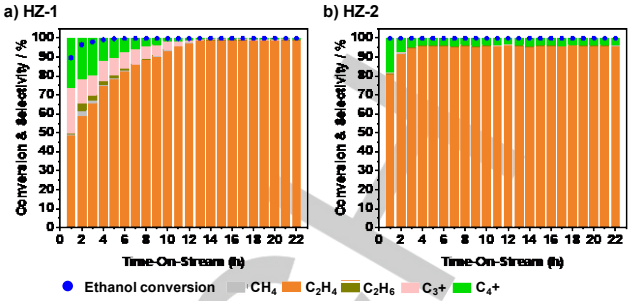

Figure 4. Ethanol conversion over HZ-1 (a) and HZ-2 (b) catalysts. The blue points indicate the conversion of ethanol. Conditions: Dehydated catalysts (0.1 g) were loaded in a fixed-bed quartz reactor under flowing nitrogen gas at 500 °C for 1 h. Reaction was carried out at 500 °C with an ethanol feeding rate of 0.64 mL/h and corresponding weight hourly space velocity (WHSV) of 5 h^{-1}.

A long unsteady-state period is often observed by using H-ZSM-5 zeolite in ethanol dehydration reactions,[7b, 7d, 36] as observed with HZ-1 zeolite. Comparing to HZ-1 zeolite, HZ-2 zeolite processes a much lower Brønsted acidity as shown in Fig. S3, however, obtained a remarkably shorter unsteady-state. The main difference between HZ-1 and HZ-2 zeolites is the presence of larger amount of tri-coordinated Al^{3+} species in HZ-2 zeolite as described above. In the catalytic dehydration of ethanol at high temperature, previous work reported that BAS are active sites, while the presence of EFAl species induces the side-reaction such as aromatics formation.[34b] However, the introduction of the dominant Al^{3+} species into zeolite in this research showed the extremely high selectivity to ethylene and nearly no unsteady-state period. Therefore, the reaction mechanism should be different after introducing strong Lewis acidic Al^{3+} species.

For the mechanistic investigation, the chemical compounds on HZ-1 and HZ-2 zeolites at the unsteady-state within different reaction time in the TOS experiments have been investigated by ^{13}C HPDEC and ^{1}H MAS NMR experiments. As shown in Fig. 5a and b, signals in the range of 127~135 ppm are assigned to carbon atoms at aromatic rings.[20, 37] No ketones or aldehydes having signals in the range of 200~220 ppm was detected.[38] The signals at 58.5 and 15 ppm were assigned to methylene and methyl groups in ethanol, respectively, indicating the existence of adsorbed ethanol.[39] On H-form zeolites, the formation of ethoxy species at BAS and terminal ethoxy species and/or strongly bonded ethanol are probed with signals at 72.6 and 61.7 ppm, respectively.[19b, 20] Ethoxy groups can be converted into ethanol upon humidity at room temperature,[19b] which could be the reason for the absence of methylene carbon signal of ethoxy groups here.

Broad weak signals at 78~85 ppm was also detected together with the signal at 27 and 11 ppm in Fig. 5b, which were assigned to oligomeric alkoxy species and the methylene and terminal methyl carbons of alkoxy species, respectively. The formation of oligomeric alkoxy species are due to the fast oligomerization of ethylene to oligomeric alkoxy species at BAS, which has been observed in the conversion of ethanol at 250 °C and can be transformed into aromatics at higher temperature.[19b] These assignments are confirmed in corresponding ^{1}H MAS NMR studies. As shown in Fig. 5c and d, the broad signals at 0.7 and 3.2 ppm were ascribed to the terminal methyl groups and the

methylene groups in ethanol, respectively. The signals at ca. 3.9 and 1.8 ppm were attributed to the methylene groups with and without connection to OH groups in C_3+ alcohols. The signals at 4.4~4.8 ppm are attributed to the hydroxyl groups in alcohols. The hydrogens bounded to aromatic rings caused the signal at 6.7 ppm.

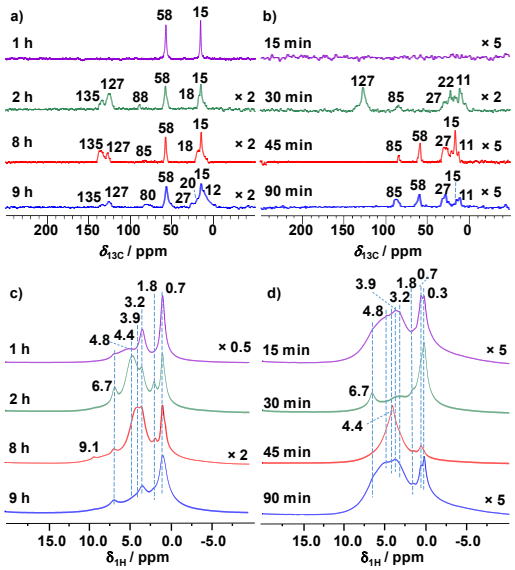

Figure 5. ^{13}C (a,b) and ^{1}H (c,d) MAS NMR spectra of reacted HZ-1 (a,c) and HZ-2 (b,d) zeolites at the unsteady-state at different time. Conditions: Dehydated catalysts (0.1 g) were loaded in a fixed-bed quartz reactor under flowing nitrogen gas at 500 °C for 1 h. Reaction was carried out at 500 °C with an ethanol feeding rate of 0.64 mL/h and corresponding WHSV of 5 h^{-1}.

On HZ-1 zeolite, the strong alcohol signal was observed throughout the unsteady-state period even after 9 h reaction time. The strong signals at δ_{13C} = 58 and 15 ppm with δ_{1H} = 0.7, 3.2 and 4.4 ppm (Fig. 5a and c) indicates that a large amount of ethanol was adsorbed on HZ-1 even after 2 h reaction, however, nearly no strong alcohol signals can be detected on HZ-2 after 15 min reaction. It indicates that the presence of EFAl-Al^{3+} remarkably enhance the conversion of ethanol to ethylene on HZ-2. On HZ-1, after 8 h reaction, the signal at δ_{1H} = 3.9 assigned to methylene carbon in higher alcohols strongly enhanced. The formation of higher alcohols in the channels of HZ-1 results in the hydroxyl protons involved in hydrogen bonds between alcohol molecules and the zeolite framework, giving a signal at δ_{1H} = 9.1 ppm. After 9 h reaction, HZ-1 almost reached the steady-state period. The signals of higher alcohols were strongly decreased (Fig. 5c), and the adsorbed alcohols became dominant, which indicates HZ-1 surface is dominated by ethoxy groups as often proposed for H-form zeolites at the steady-state period.[34] The presence of BTX (Benzene, toluene, xylene) is observed at the very beginning and throughout the reaction period at δ_{13C} = 135~127 and 18~20 ppm together with the signal at δ_{1H} = 6.7 ppm.

On HZ-2 zeolite, a new signal at δ_{1H} = 0.3 ppm was detected after 15 min reaction (Fig. 5d), which was not detected on both dehydrated zeolites, as well as on HZ-1 during ethanol dehydration. The signal at δ_{1H} = 0.3 ppm hints to the formation of AlOH groups, which can be formed by the abstraction of hydroxyl groups of ethanol at EFAl-Al^{3+} sites as proposed in Scheme S2b. Therefore, the ethoxy group is generated on HZ-2 surface during the reaction. In terms of the high selectivity to ethylene and the ethoxy groups are recognized as the key intermediates in the formation of ethylene under current conditions, a high content of ethoxy groups was considered to be generated on HZ-2 after 15 min reaction. After 30 min reaction, the content of alcohols remarkably reduced and the spectrum (Fig. 5d) is dominated by an AlOH signal at δ_{1H} = 0.3 ppm with a weak signal at δ_{1H} = 6.7 ppm of aromatic hydrogen. The formation of aromatics on HZ-2 after 30 min reaction was also confirmed in Fig. 5b.

Compared to ethanol dehydration on HZ-1, only very weak alcohol signals can be detected on HZ-2 in Fig. 7b, hinting the rapid conversion of ethanol on HZ-2, which has been confirmed by the reaction results in Fig. S5 and Fig. 4. The lack of higher alcohol signals confirms the higher ethylene selectivity shown in Fig. 4. Notably, the signals at δ_{13C} = 85 and 27 ppm indicates the formation of oligomeric alkoxy species, which can be transformed into aromatics, showing a strong signal at δ_{13C} = 127 ppm with a broad signal at 11~22 ppm due to the wide distribution of methyl and methylene carbon bonded to aromatics. AlOH groups was almost disappeared after 45 min reaction, while the signal at δ_{1H} = 4.4 ppm became dominant. In terms of the very weak terminal methyl carbon signal at δ_{1H} = 0.7 ppm, the strong broad signal at δ_{1H} = 4.4 ppm was caused by the conversion of ethoxy and oligomeric alkoxy species into corresponding alcohols, which is confirmed by the corresponding ^{13}C NMR experiment showing clear alcohol signals. The content of oligomeric alkoxy species simultaneously increased with reaction proceeding after 90 min reaction. Again, relative strong ethanol and AlOH signals was observed in ^{1}H NMR spectrum after 90 min reaction, similarly to that observed after 15 min reaction, while a significant increase of oligomeric alkoxy species with weak alcohol signals were detected. The absence of aromatics after 30 min reaction indicates the catalytic cycle on HZ-2 is not only dependent from the formation of aromatics, which is different from carbon pool mechanism proposed in methanol-to-olefin (MTO) reactions.[37, 40] These observation indicates that introducing Al^{3+} species on HZ-2 could facilitate the direct ethanol dehydration with a very short unsteady-state period, compared to those observed with HZ-1 without tri-coordinated Al^{3+} species, on which the complicated formation of long chain alcohols and aromatics in the unsteady-state period was observed.

At the steady-state period, both direct and indirect ethanol dehydration mechanisms are proposed for EFAl species (LAS) as those proposed for BAS (Scheme S1),[8d, 34a, 39] but exhibit a lower activity than BAS in literature.[41] In this work, we show that introducing tri-coordinated Al^{3+} species could achieve the high ethanol conversion and ethylene selectivity and reach the steady-state period in a short term. The proposed reaction mechanism has been summarized.

Discussion of Reaction Mechanisms over H-ZSM-5 zeolites. Our experimental observations indicate introducing tri-coordinated Al^{3+} species can accelerate the cleavage of C-OH bond and promote the rapid formation of ethylene at high selectivity. A possible reaction network for ethanol dehydration to ethylene on H-ZSM-5 with the collaboration of tri-coordinated Al^{3+} species and BAS was proposed (Fig. 6). Carbenium ions formed

by OH abstraction at Al^{3+} sites (route 1) are highly unstable, which are easily decomposed into ethylene or be evolved to form ethoxy groups in the local Si-O-Al sites (route 2). In HZ-2, due to the fast conversion of ethanol at Al^{3+} sites, the high concentration of ethylene inside the zeolite channels can be reacted with bridging OH groups, resulting in ethoxy groups as well (route 11). In addition, the ethylene are able to be transformed into oligomeric alkoxy species (δ_{13C} =80~88 ppm), higher olefins or alcohols via oligomerization, alkylation and cracking (route 3, 12, 13, 14).[42] In the unsteady-state period, HZ-1 containing mainly BAS is less effective in the conversion of ethanol compared to HZ-2 having Al^{3+} species. The high concentration of ethanol inside channels is potential for react with ethylene via electrophilic addition in the presence of strong BAS on HZ-1, which results in the high concentration of C_3+ alkene as observed in Fig. 4 via dehydration of higher alcohols. With reaction proceeding, the high content of ethylene and carbenium ions promote the hydride abstraction and the aromatization of oligomeric alkoxy species and higher olefins, leading to rapid formation of aromatics (δ_{13C} = 127 ppm) after 30 min reaction on HZ-2 (route 4).[7h, 36] For comparison, the formation of aromatics (δ_{13C} =127~135 ppm) on HZ-1, was only observed after 2 h reaction, which having almost twice more BAS for oligomerization and aromatization. This is in agreement with previously reported on H-ZSM-5 that the presence of strong LAS in high content can facilitate the formation of aromatics.[34b] The formation aromatics are widely accepted as carbon pool intermediates to promote the generation of carbenium ions. Here, aromatics, including benzene, toluene, xylene and 4-ethyltoluene, are possible intermediates for aromatics-based cycle to produce ethylene and methylbenzenes.[42] BTX has been considered as the intermediate for ethylene production and the formation of polymethylbenzenes intermediates in MTO reactions,[37, 42b] which can stabilize the carbenium ions and act as active species for hydrocarbon reaction.

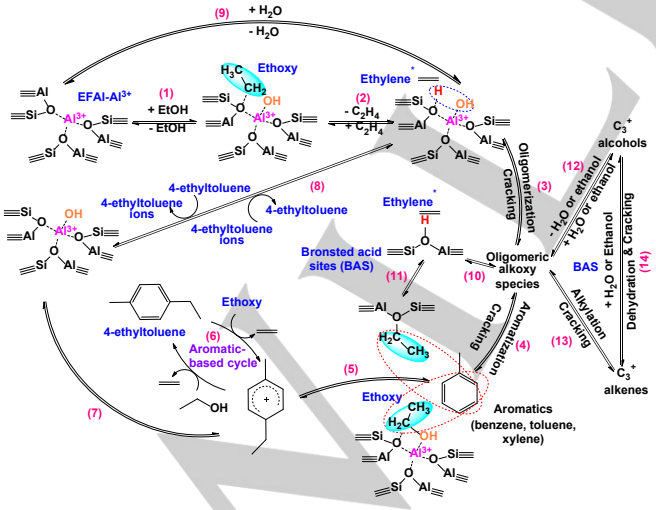

Figure 6. Proposed reaction network for ethanol dehydration on H-ZSM-5.

Here, a significant amount of BTX was generated in HZ-2 after 30 min reaction, but no significant BTX could be detected significant until after 2 h reaction in HZ-1. 4-ethyltoluene could be produced with BTX by the alkylation of aromatics with ethoxy groups or ethylene (route 5). It should be noted that the stability of alkylcarbenium ions increases in the series primary < secondary < tertiary and also depends on the local electrostatic field in zeolites.[43] Therefore, ethoxy groups and aromatics are working together for the ethanol dehydration, since aromatics are ideal proton acceptors due to their high electron density, which can be stabilized and undergo deprotonation during catalytic reactions, such as those reported in ethylbenzene disproportionation reactions.[44] Therefore, an aromatics-based cycle (route 6) has been proposed to explain the high activity of HZ-2 compared to HZ-1. As shown in route 6, the attack of ethoxy groups to aromatics results in ethylbenzene ions and release ethylene, which can also contribute protons to another ethanol molecule for dehydration to ethylene.

Conclusion

In this work, H-ZSM-5 zeolites without (HZ-1) and with (HZ-2) the introduction of tri-coordinated extra-framework Al^{3+} (EFAl-Al^{3+}) species were prepared for catalytic dehydration of ethanol to ethylene. The detection of invisible Al^{3+} species in dehydrated HZ-2 zeolite has been achieved by ^{27}Al MAS MQNMR experiments upon water loading, which revealed the presence of dominant EFAl-Al^{3+}species on HZ-2, while nearly no EFAl species can be detected on HZ-1. The existence and the densities of both BAS (bridging OH groups) and LAS (Al cations) were characterized by ^{1}H and ^{31}P MAS NMR investigations. Co-existence of a large content of LAS with a similar amount of BAS (bridging OH groups) is observed on HZ-2, while HZ-1 consists mainly BAS.

HZ-2 with tri-coordinated Al^{3+} species, is highly active through the whole temperature range, providing a high ethylene selectivity (> 95 %) at the complete conversion of ethanol above 300 °C. At 500 °C, however, a high selectivity to ethylene (> 95 %) at a nearly complete conversion of ethanol was achieved on HZ-1 without tri-coordinated Al^{3+} species. HZ-2 requires much shorter unsteady-state period of 1~2 h compared to 9 h on HZ-1 in obtaining a high ethylene selectivity at steady-state ethanol conversion. The excellent catalytic performance has been attributed to the presence of tri-coordinated Al^{3+} species, which collaborates with BAS in the reaction on HZ-2. The strong Lewis acidic Al^{3+} species can facilitate the fast hydroxyl abstraction from ethanol to produce ethylene, or promote the formation of oligomeric alkoxy species, resulting in aromatics via secondary reaction on BAS. The aromatics with high electron density can promote the production of ethylene via an aromatics-based cycle from ethanol, which offers an alternative route to the indirect ethanol dehydration on zeolites. The elucidation of the effect of tri-coordinated extra-framework Al species provides a better understanding of bioethanol-to-ethylene catalysis, which is important for replacing petroleum and coal for the sustainable production of industrial favourite ethylene.

Acknowledgements

This work was supported by the Australian Research Council Discovery Projects (DP150103842) and Discovery Earlier Career Research Project (DE190101618), the SOAR Fellowship, and the Sydney Nano Grand Challenge from the University of Sydney from the University of Sydney.

Keywords: MFI zeolite • acidity • tri-coordinated aluminium • solid-state NMR spectroscopy • ethanol-to-olefin

[1] 232nd ACS National Meeting. *Chem. Eng. News Archive* **2006,** *84*, 59-236.

[2] *The Ethylene Technology Report 2016,* Research and Markets: Dublin, Ireland, 19 June **2016**.

[3] I. Amghizar, L. A. Vandewalle, K. M. Van Geem, G. B. Marin, *Eng.* **2017,** *3*, 171-178.

[4] H. Zabed, J. N. Sahu, A. Suely, A. N. Boyce, G. Faruq, *Renew. Sust. Energ. Rev.* **2017,** *71*, 475-501.

[5] D. P. Liu, Y. Liu, E. Y. L. Goh, C. J. Y. Chu, C. G. Gwie, J. Chang, A. Borgna, *Appl. Catal. A-Gen.* **2016,** *523*, 118-129.

[6] J. Sun, Y. Wang, *ACS Catal.* **2014,** *4*, 1078-1090.

[7] (a) R. Le Van Mao, P. Levesque, G. McLaughlin, L. H. Dao, *Appl. Catal.* **1987,** *34*, 163-179; (b) C. B. Phillips, R. Datta, *Ind. Eng. Chem. Res.* **1997**, *36*, 4466-4475; (c) R. Le Van Mao, T. M. Nguyen, G. P. McLaughlin, *Appl. Catal.* **1989,** *48*, 265-277; (d) J. Bi, X. Guo, M. Liu, X. Wang, *Catal. Today* **2010**, *149*, 143-147; (e) K. A. Tarach, J. Tekla, U. Filek, A. Szymocha, I. Tarach, K. Gora-Marek, *Microporous Mesoporous Mater.* **2017**, *241*, 132-144; (f) T. K. Phung, L. P. Hernandez, A. Lagazzo, G. Busca, *Appl. Catal. A-Gen.* **2015**, *493*, 77-89; (g) R. Le Van Mao, T. M. Nguyen, J. Yao, *Appl. Catal.* **1990,** *61*, 161-173; (h) M. Inaba, K. Murata, M. Saito, I. Takahara, *React. Kinet. Catal. Lett.* **2006,** *88*, 135-141; (i) H. Xin, X. Li, Y. Fang, X. Yi, W. Hu, Y. Chu, F. Zhang, A. Zheng, H. Zhang, X. Li, *J. Catal.* **2014,** *312*, 204-215; (j) K. K. Ramasamy, Y. Wang, *Catal. Today* **2014**, *237*, 89-99.

[8] (a) H. D. Zhu, A. Ramanathan, J. F. Wu, B. Subramaniam, *ACS Catal.* **2018**, *8*, 4848-4859; (b) M. J. Janik, J. Macht, E. Iglesia, M. Neurock, *The J. Phys. Chem. C* **2009,** *113*, 1872-1885; (c) M. C. H. Clemente, G. A. V. Martins, E. F. de Freitas, J. A. Dias, S. C. L. Dias, *Fuel* **2019**, *239*, 491-501; (d) D. Li, P. Bui, H. Y. Zhao, S. T. Oyama, T. Dou, Z. H. Shen, *J. Catal.* **2012,** *290*, 1-12.

[9] W. R. Moser, R. W. Thompson, C. C. Chiang, H. Tong, *J. Catal.* **1989,** *117*, 19-32.

[10] Y. Jiang, J. Huang, W. Dai, M. Hunger, *Solid State Nucl. Magn. Reson.* **2011,** *39*, 116-141.

[11] F. F. Madeira, K. Ben Tayeb, L. Pinard, H. Vezin, S. Maury, N. Cadran, *Appl. Catal. A-Gen.* **2012,** *443*, 171-180.

[12] (a) C. Y. Wu, H. S. Wu, *ACS Omega* **2017**, *2*, 4287-4296; (b) Q. Y. Meng, H. C. Xin, Y. F. Zhang, Y. Huang, X. F. Yi, Y. Y. Sun, S. F. Zhong, X. B. Li, *Sci. Adv. Mater.* **2015**, *7*, 2343-2351.

[13] (a) X. Yi, K. Liu, W. Chen, J. Li, S. Xu, C. Li, Y. Xiao, H. Liu, X. Guo, S.-B. Liu, A. Zheng, *J. Am. Chem. Soc.* **2018,** *140*, 10764-10774; (b) Z. Yu, A. Zheng, Q. Wang, L. Chen, J. Xu, J. P. Amoureux, F. Deng, *Angew. Chem. Int. Ed.* **2010,** *49*, 8657-8661.

[14] (a) J. Jiao, J. Kanellopoulos, W. Wang, S. S. Ray, H. Foerster, D. Freude, M. Hunger, *Phys. Chem. Chem. Phys.* **2005,** *7*, 3221-3226; (b) J. Jiao, J. Kanellopoulos, B. Behera, Y. J. Jiang, J. Huang, V. R. R. Marthala, S. S. Ray, W. Wang, M. Hunger, *J. Phys. Chem. B* **2006,** *110*, 13812-13818; (c) S. H. Li, A. M. Zheng, Y. C. Su, H. J. Fang, W. L. Shen, Z. W. Yu, L. Chen, F. Deng, *Phys. Chem. Chem. Phys.* **2010,** *12*, 3895-3903.

[15] S. P. Brown, H. W. Spiess, *Chem. Rev.* **2001,** *101*, 4125-4156.

[16] Z. Yu, S. Li, Q. Wang, A. Zheng, X. Jun, L. Chen, F. Deng, *J. Phys. Chem. C* **2011,** *115*, 22320-22327.

[17] H. M. Kao, C. P. Grey, *J. Am. Chem. Soc.* **1997,** *119*, 627-628.

[18] M. A. Christiansen, G. Mpourmpakis, D. G. Vlachos, *ACS Catal.* **2013**, *3*, 1965-1975.

[19] (a) S. A. Kadam, M. V. Shamzhy, *Catal. Today* **2018**, *304*, 51-57; (b) W. Wang, J. Jiao, Y. J. Jiang, S. S. Ray, M. Hunger, *ChemPhysChem* **2005**, *6*, 1467-1469.

[20] C. Wang, Y. Chu, J. Xu, Q. Wang, G. Qi, P. Gao, X. Zhou, F. Deng, *Angew. Chem. Int. Ed.* **2018,** *57*, 10197-10201.

[21] J. P. Amoureux, C. Fernandez, S. Steuernagel, *J. Magn. Reson., Ser A* **1996,** *123*, 116-118.

[22] (a) H. Sang, H. Y. Chu, J. H. Lunsford, *Catal. Lett.* **1994**, *26*, 235-246; (b) S. Beran, P. Jiru, B. Wichterlova, *J. Phys. Chem.* **1981,** *85*, 1951-1956

[23] Z. C. Zhao, S. C. Xu, M. Y. Hu, X. H. Bao, C. H. F. Peden, J. Z. Hu, *J. Phys. Chem. C* **2015,** *119*, 1410-1417.

[24] (a) B. H. Wouters, T. H. Chen, P. J. Grobet, *J. Am. Chem. Soc.* **1998,** *120*, 11419-11425; (b) E. Bourgeatlami, P. Massiani, F. Direnzo, P. Espiau, F. Fajula, T. D. Courieres, *Appl. Catal.* **1991,** *72*, 139-152.

[25] A. Zheng, S. B. Liu, F. Deng, *Chem. Rev.* **2017**, *117*, 12475-12531.

[26] E. F. Rakiewicz, A. W. Peters, F. Wormsbecher, K. J. Sutovich, K. T. Mueller, *J. Phys. Chem. B* **1998,** *102*, 2890-2896.

[27] S. Lang, M. Benz, U. Obenaus, R. Himmelmann, M. Hunger, *ChemCatChem* **2016**, *8*, 2031-2036.

[28] A. Zheng, S. J. Huang, S. B. Liu, F. Deng, *Phys. Chem. Chem. Phys.* **2011,** *13*, 14889-14901.

[29] S. Li, A. Zheng, Y. Su, H. Zhang, L. Chen, J. Yang, C. Ye, F. Deng, *J. Am. Chem. Soc.* **2007,** *129*, 11161-11171.

[30] (a) J. Huang, N. van Vegten, Y. Jiang, M. Hunger, A. Baiker, *Angew. Chem. Int. Ed.* **2010,** *49*, 7776-7781; (b) Z. C. Wang, Y. J. Jiang, O. Lafon, J. Trebosc, K. D. Kim, C. Stampfl, A. Baiker, J. P. Amoureux, J. Huang, *Nat. Commun.* **2016,** *7*, 13820.

[31] R. J. S. Francis A. Carey, *Advanced Organic Chemistry*. Springer: USA, **2007**.

[32] E. M. Arnett, T. C. Hofelich, *J. Am. Chem. Soc.* **1983,** *105*, 2889-2895.

[33] J. N. Kondo, H. Yamazaki, R. Osuga, T. Yokoi, T. Tatsumi, *J. Phys. Chem. Lett.* **2015**, *6*, 2243-2246.

[34] (a) A. P. Kagyrmanova, V. A. Chumachenko, V. N. Korotkikh, V. N. Kashkin, A. S. Noskov, *Chem. Eng. J.* **2011,** *176*, 188-194; (b) I. Rossetti, M. Compagnoni, E. Finocchio, G. Ramis, A. Di Michele, Y. Millot, S. Dzwigaj, *Appl. Catal. B-Environ.* **2017,** *210*, 407-420.

[35] K. Larmier, C. Chizallet, S. Maury, N. Cadran, J. Abboud, A. F. Lamic-Humblot, E. Marceau, H. Lauron-Pernot, *Angew.Chem. Int. Ed.* **2017,** *56*, 230-234.

[36] Z. S. B. Sousa, C. O. Veloso, C. A. Henriques, V. Teixeira da Silva, *J. Mol. Catal. A: Chem. **2016,** 422, 266-274.*

[37] Q. Q. Peng, G. T. Wang, Z. C. Wang, R. L. Jiang, D. Wang, J. F. Chen, J. Huang, *ACS Sustain. Chem. Eng.* **2018**, *6*, 16867-16875.

[38] Z. Wang, J. Huang, R. Amal, Y. Jiang, *Appl. Catal. B-Environ.* **2018,** *223*, 16-21.

[39] X. Zhou, C. Wang, Y. Chu, J. Xu, Q. Wang, G. Qi, X. Zhao, N. Feng, F. Deng, *Nat. Commun.* **2019,** *10*, 1961.

[40] C. Wang, J. Xu, G. Qi, Y. Gong, W. Wang, P. Gao, Q. Wang, N. Feng, X. Liu, F. Deng, *J. Catal.* **2015,** *332*, 127-137.

[41] C. P. Nash, A. Ramanathan, D. A. Ruddy, M. Behl, E. Gjersing, M. Griffin, H. D. Zhu, B. Subramaniam, J. A. Schaidle, J. E. Hensley, *Appl. Catal. A-Gen.* **2016**, *510*, 110-124.

[42] (a) S. Svelle, F. Joensen, J. Nerlov, U. Olsbye, K. P. Lillerud, S. Kolboe, M. Bjørgen, *J. Am. Chem. Soc.* **2006,** *128*, 14770-14771; (b) M. Bjørgen, S. Svelle, F. Joensen, J. Nerlov, S. Kolboe, F. Bonino, L. Palumbo, S. Bordiga, U. Olsbye, *J. Catal.* **2007,** *249*, 195-207.

[43] J. Huang, Y. Jiang, V. R. R. Marthala, M. Hunger, *J. Am. Chem. Soc.* **2008,** *130*, 12642-12644.

[44] J. Huang, Y. J. Jiang, V. R. R. Marthala, W. Wang, B. Sulikowski, M. Hunger, *Microporous Mesoporous Mater.* **2007**, *99*, 86-90.

Tri-coordinated Al^{3+} species working with Brønsted acid sites can accelerate bioethanol dehydration at the much lower reaction temperature and short unsteady-state period from > 9 h to 1~2 h.

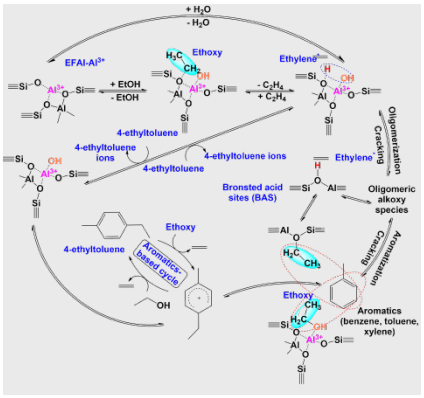

*Zichun Wang, Luke A. O'Dell, Xin Zeng, Can Liu, Shufang Zhao, Wenwen Zhang, Yijiao Jiang, and Jun Huang**

Page No. – Page No.

Insight into Tri-coordinated Aluminium Species on Ethanol-to-Olefin Conversion over ZSM-5 Zeolites